STRUCTURES AND MECHANISMS OF LIPID PHASE TRANSITIONS IN NONAQUEOUS MEDIA

Dipalmitoylphosphatidylethanolamine in Fused Salt

W. TAMURA-LIS, L. J. LIS, AND P. J. QUINN*
Department of Physics and the Liquid Crystal Institute, Kent State University, Kent, Ohio 44242; and
**Department of Biochemistry, King's College London, Kensington Campus, London W8 7AH United Kingdom*

ABSTRACT The phase transitions for dipalmitoylphosphatidylethanolamine (DPPE) dispersed in water and in *N*-ethylammonium nitrate (EAN) were examined using differential scanning calorimetry and time-resolved x-ray diffraction. Subgel, pre-, and main-phase transitions were observed for DPPE in water, whereas only the pre-and main transitions were observed for DPPE in EAN. Hysteresis was observed for both dispersions upon cooling. In addition, the lamellar (L_α) to hexagonal (H_α) phase transition was observed for DPPE dispersed in EAN when using time-resolved x-ray diffraction but not when using calorimetry. This low enthalpy process occurred at 73–77°C, which is significantly lower than that observed for DPPE in water. The presence of EAN stabilizes the existence of the H_α phase in DPPE by its influence on the bilayer interfacial properties, primarily on the area per lipid head group.

INTRODUCTION

The role of water in the stability of phospholipid structures, phase transitions, and interactive forces between and within structures is a topic of current concern when defining the role of solvation in membranes. One of the approaches in recent years has involved the substitution of water by other solvents (1–6), and characterization of the differences resulting from observations of phospholipid properties. A trend has emerged indicating that solvents which change the interactive forces between molecules within a bilayer with a concomitant change in the area per head group, can lead those molecules to form interdigitated bilayer phases (1, 4, 7) or even nonlamellar structures (8). The correlation between specific structures and an easily characterized property of the solvent is still in the exploratory stage.

In a related subfield, the relationship between area per head group (expressed as the radius of curvature) and the packing of acyl chains, to the lamellar to hexagonal II phase transition has been discussed independently by Siegel (9) and Gruner (10). Specifically, the balance between the head group area and the acyl chain void volume is a determining factor in the tendency of a lipid to form either the lamellar or the hexagonal II phase. The influence of hydrocarbon molecules and phospholipid head groups on the stability of the hexagonal II phase has been discussed elsewhere (11). However, a recent report has shown that the spreading of lipid head groups due to solvent structure can also lead to the greater stability of a nonlamellar phase (8). The unique aspect of this observation was that (DPPC) molecules which do not form non-lamellar phases in water were induced to form an H_{II} phase in the presence of the fused salt, ethylammonium nitrate. Thus, using EAN allows one to observe the effect of spreading lipid molecules (i.e., increasing the area per head group) on the lamellar to H_{II} transition without having to add molecules to the lipid bilayer because this addition may provide an impetus for the formation of the H_{II} phase all or in part by the ability of the molecules to fill void spaces within the H_{II} hydrocarbon space.

The present study was undertaken to investigate the influence of EAN when it is substituted for water as the solvation media for L-DPPE molecules. Calorimetry and time-resolved x-ray diffraction experiments were used to investigate the various transformations between lamellar and nonlamellar structures in this system. Particular attention was paid to the possibility that EAN provides a favorable environment for the DPPE molecules to form an H_{II} phase whereas DPPE in water has been shown to undergo an L_α to H_{II} transition at ~123°C (12). Analysis of the data also provides information about the structures involved in the transitions.

MATERIALS AND METHODS

The 1,2 L-α-dipalmitoylphosphatidylethanolamine (DPPE) was obtained from Fluka A.G. (Buchs, Switzerland) and Avanti Polar Lipids (Birmingham, AL), and used without further purification. The *N*-ethylammonium nitrate (EAN) was a gift of Prof. Barry Ninham. The preparation of EAN has been described in Evans et al. (13). Lipid dispersions were prepared by suspending the DPPE in water or in EAN at ~80°C until a uniform liquid crystalline phase was observed. All dispersions were

then equilibrated at 0°C for 4–5 d. Samples for calorimetric measurements were sealed in aluminum pans, whereas those for x-ray diffraction measurements were mounted between mica sheets.

Differential scanning calorimetry was performed using a DSC-2C (Perkin-Elmer Corp., Norwalk, CT) with an Intracooler II for low temperature equilibration. All scans of 10°C · min^{-1} were begun at 2°C and terminated at 87°C. Data recording and analysis were obtained using a Perkin-Elmer Data Station interfaced with the calorimeter.

X-ray experiments were carried out using the monochromatic (0.150 nm) focused x-ray beam at Station 7.2/3 of the Daresbury Synchrotron Laboratory as previously described (14). A cylindrically bent single crystal of Ge (15) and a long float mirror were used for monochromatization and horizontal focusing, providing 2×10^9 photons · s^{-1} down a 0.2-mm collimator at 2.0 GeV and 100–200 mA of electron beam current. A Keele flat plate camera was used with a linear detector constructed at Daresbury. The dead time between 1.5 s data acquisition frames was 50 ms. X-ray scattering was recorded using a linear detector fabricated at the Daresbury Lab and was calibrated using Teflon (0.48 nm) as a standard (16). Plots were typically recorded first as a function of tan 2θ and then replotted in reciprocal space ($S = 2 \sin\theta/\lambda$) for publication. All mesophase and subcell spacings were calculated using Bragg's Law as previously described (17).

Temperature scans were produced by water baths connected internally to the sample mount of the x-ray camera. The temperature of the sample was monitored internally using a thermocouple placed adjacent to the sample in the x-ray sample holder.

RESULTS AND DISCUSSION

The phases and phase transitions for DPPE in water have been the subject of numerous studies (12, 18–23). In general, it was found that the transition between the crystalline bilayer (L_c) and liquid crystalline bilayer (L_α) phases was hysteretic with the formation of a metastable gel state bilayer (L_β) upon cooling from the L_α phase. The longer the sample was equilibrated in the L_α phase, the longer the L_β phase was stable upon subsequent cooling before the final relaxation into the L_c state. Structural parameters have been determined for both the L_β and L_α phases (20, 21).

The phase history of a sample of DPPE in 80 wt% water, which was equilibrated at 0°C for 4–5 d, was monitored using differential scanning calorimetry (Fig. 1). The initial heating scan indicated that the sample was able to undergo a subgel transition at 23°C, a pretransition at 36°C, and a main transition with the L_α phase as the final state at 63°C. This result is consistent with previous examinations of the phases present in DPPE/water as a function of temperature. Although the lamellar (L_α) to hexagonal (H_α) phase transition has been previously shown to occur at ~123°C (12), our sample was not heated above 87°C to minimize the chance of sample damage during the liquid to vapor transition for water at 100°C. The L_α to L_β phase transition was observed at 62°C upon cooling with a reduction (of 5–10%) in the transition enthalpy of the main transition observed during initial heating, and the L_β to L_α phase transition was observed at 63°C upon reheating with a further reduction (of 5–10%) in the transition enthalpy on cooling. The apparent 1°C supercooling for the L_α to L_β phase transition is probably an artifact of the rate at which the temperature was scanned.

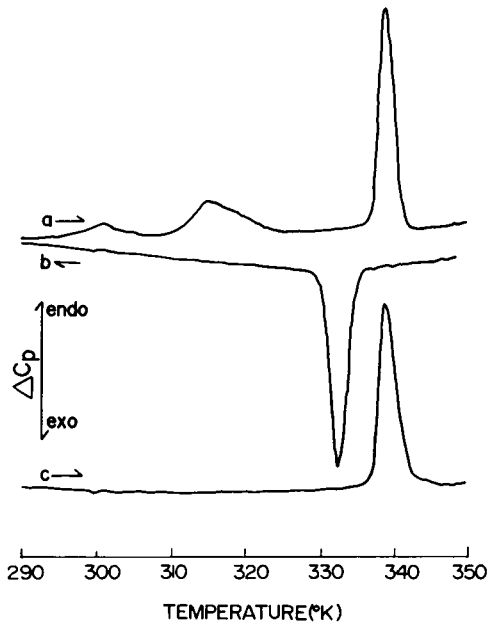

FIGURE 1 Thermograms for DPPE in water after equilibration at 4°C for 5 d to induce the subgel phase. (*a*) Initial heating. (*b*) Initial cooling. (*c*) First reheating. The temperature was scanned at a rate of 10°C · min^{-1}.

A similar set of calorimetry experiments was run with a sample of 20% wt/vol DPPE dispersed in EAN (Fig. 2). The initial heating scan indicated that the sample underwent a pretransition at 39°C and a main transition to the L_α phase at 67°C. These temperature values are similar to those observed for the same transitions in DPPE in water. The slight increase in transition temperature upon heating may indicate that the DPPE bilayers are more ordered (i.e., closer packed) for the same phase in EAN than in water; this is consistent with similar observations in phosphatidylcholines (8, 13, 24). The lack of a subtransition may be due to the DPPE molecules decreasing their attraction for each other within a bilayer because of the substitution of a concentrated salt for water. This phenomenon would allow for a spreading of the DPPE head groups with a concomitant decrease in the packing of the acyl chains within the bilayer. The initial bilayer state would be less ordered (i.e., less close packed) for DPPE bilayers in EAN when compared with bilayers in water. This conclusion is also consistent with observations reported for phosphatidylcholines in water and EAN (18). A simple alternative explanation is that the subtransition enthalpy is too small for DPPE dispersed in EAN to be registered by the calorimeter. This is a less likely explanation because the fast scan rate would tend to enhance the observation of a phase transition thermogram. The transition between the liquid crystal and L_β phases occurs at 64°C upon cooling, and the reverse transition occurs at 67°C upon reheating. The transition enthalpies for these transitions were 10–20% greater than that observed upon initial heating. No other phase transitions are observed in the heating and

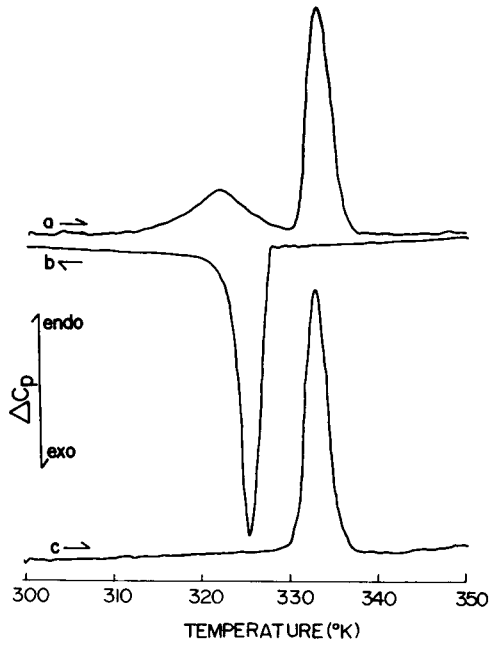

FIGURE 2 Thermograms for DPPE in fused salt after equilibration at 4°C for 5 d. (*a*) Initial heating. (*b*) Initial cooling. (*c*) First reheating. The temperature was scanned at a rate of 10°C · min^{-1}.

cooling scans with 2°C and 87°C being the lower and upper limits. The slight supercooling observed for the sample upon cooling is again probably an artifact of our scan rate.

An overview of the structural changes that occur for DPPE dispersed in EAN during heating and cooling was obtained by recording consecutive x-ray diffraction patterns at ~1.5-s intervals throughout the phase transitions (Figs. 3 and 4). Our examination of the $L_\beta \rightleftharpoons L_\alpha$ transition for DPPE in water is reported elsewhere (Tenchov, B., L. J. Lis, and P. J. Quinn. Submitted for publication). Wide angle diffraction peaks were not resolvable during the heating or cooling scans. This low resolution may be due to our use of an area detector, small domains of DPPE molecules within the bilayer and/or highly directionally oriented acyl chain packing. Thus all phase assignments are tentative with regards to the acyl chain packing until wide angle diffraction peaks are obtained. The crystalline or low-temperature phase for DPPE in EAN produces a small angle x-ray diffraction pattern which can be indexed as due to a lamellar structure with a repeat spacing of 52.6 Å. As the temperature is scanned above 70°C, there is no apparent change in this repeat spacing. When the temperature is between 73 and 77°C a new small angle diffraction pattern is observed which indexes to an hexagonal array of cylinders with a repeat spacing of 55.8 Å. Although the resolution of the time-resolved x-ray experiment is not

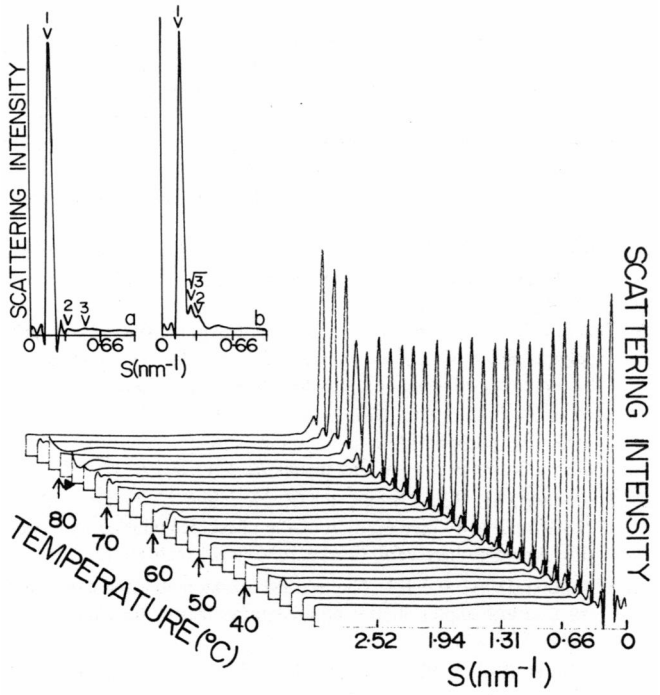

FIGURE 3 Three-dimensional plot of diffraction intensity versus reciprocal spacing as a function of temperature during the initial heating scan from 26 to 84°C at 10° · min^{-1} for DPPE in fused salt equilibrated at 5 d. Every tenth frame of a data set of 255 frames of 1.5 s duration are shown in the figure. Inserts *a* and *b* are the first and last frame, respectively, of the data set.

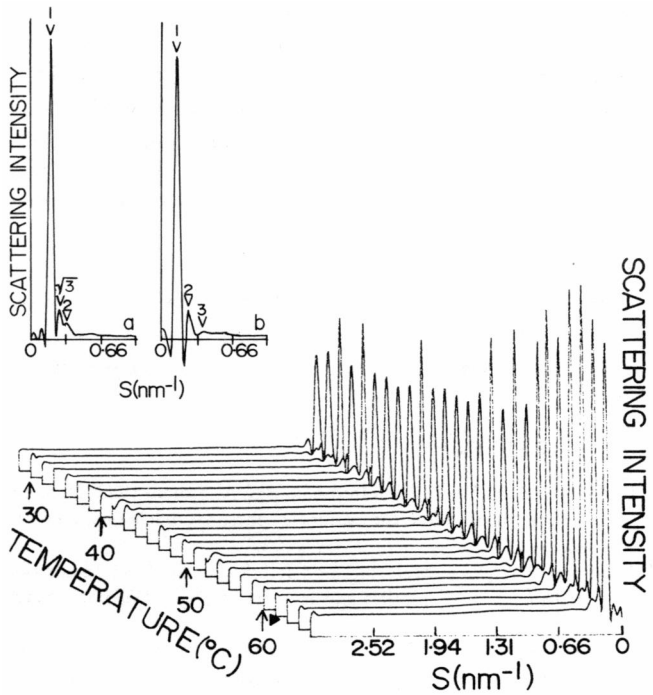

FIGURE 4 Three-dimensional plot of diffraction intensity versus reciprocal spacing as a function of temperature during the initial cooling scan from 63 to 26.5°C at 10° · min^{-1} for DPPE in fused salt. Every tenth frame of a data set of 255 frames of 1.5 s duration are shown in the figure. Inserts *a* and *b* are tracings of the first and last frame, respectively, of the data set.

sufficient to observe the various bilayer transitions recorded using calorimetry, the L_α to H_α transition which is not apparent in the calorimeter tracing can be determined. This is a significant lowering of the transition temperature (~123°C) for the L_α to H_α phase transition in DPPE dispersed in water (12).

A transition from the H_α phase is observed at ~63°C that can be inferred to be the H_α to L_β by comparison with the calorimetry results. The bilayer repeat spacing for the L_β phase is 70.4 Å which is significantly larger than that observed for DPPE in water (20). This is an indication that either the lipid molecules are packed differently within the bilayer in water versus EAN, and/or there is an increase in solvent between the bilayers. The former explanation is less likely because there is no apparent tilt for DPPE acyl chains when they are fully hydrated with water (20).

CONCLUSIONS

It has been shown that DPPE in water and EAN have a variety of phase transitions which are dependent on sample history. In addition, the presence of EAN favors the formation of nonbilayer phases as evidenced by the appearance of an H_α phase in DPPE at ~50°C lower than that inferred in water. Thermodynamic arguments have been presented by O'Leary and Levin (24) for the tendency of DPPE in EAN to form a nonlamellar phase. In the context of the conditions favoring the formation of cylindrical arrays over multilamellar arrays (10, 11), an increase in area per head group could allow for a greater intrinsic curvature as a prerequisite for cylinder formation, thus overcoming unfavorable hydrocarbon packing considerations within the mesophase. This system merits further study to determine the kinetics and high resolution structures (i.e., head group areas) of the L_α to H_α phase transition which can then be correlated with predictions from the appropriate theories (9, 10).

This research was partially supported by a grant from The Science and Engineering Research Council (United Kingdom).

Received for publication 8 December 1986 and in final form 10 December 1987.

REFERENCES

1. McDaniel, R. V., T. J. McIntosh, and S. A. Simon. 1983. Nonelectrolyte substitution for water in phosphatidylcholine bilayers. *Biochim. Biophys. Acta.* 731:97–108.
2. Simon, S. A., R. V. McDaniel, and T. J. McIntosh. 1982. Interaction of benzene with micelles and bilayers. *J. Phys. Chem.* 86:1449–1456.
3. McDaniel, R. V., S. A. Simon, T. J. McIntosh, and V. Borovyagin. 1982. Interaction of benzene with bilayers. Thermal and structural studies. *Biochemistry.* 21:4116–4126.
4. O'Leary, T. J., and I. W. Levin. 1984. Raman spectroscopic study of an interdigitated lipid bilayer: dipalmitoylphosphatidylcholine dispersed in glycerol. *Biochim. Biophys. Acta.* 776:185–189.
5. Rowe, E. S. 1983. Lipid chain length and temperature dependence of ethanol–phophatidylcholine interactions. *Biochemistry.* 22:3299–3305.
6. Simon, S. A., and T. J. McIntosh. 1984. Interdigitated hydrocarbon chain packing causes the biphasic transition behavior in lipid/alcohol suspensions. *Biochim. Biophys. Acta.* 773:169–172.
7. McIntosh, T. J., R. V. McDaniel, and S. A. Simon. 1983. Induction of an interdigitated gel phase in fully hydrated phosphatidylcholine bilayers. *Biochim. Biophys. Acta.* 731:109–114.
8. Tamura-Lis, W., L. J. Lis, and P. J. Quinn. 1987. Structures and mechanisms of lipid phase transitions in nonaqueous media: dipalmitoylphosphatidylcholine in fused salt. *J. Phys. Chem.* 91:4625–4627.
9. Siegel, D. P. 1986. Inverted micellar intermediates and the transitions between lamellar, cubic and inverted hexagonal phases. I. Mechanism of the $L_\alpha \leftrightarrow H_{II}$ phase transitions. *Biophys. J.* 49:1155–1170.
10. Gruner, S. M., 1985. Intrinsic curvature hypothesis for biomembrane lipid composition: a role for nonbilayer lipids. *Proc. Natl. Acad. Sci. USA.* 82:3665–3669.
11. Kirk, G. L., and S. M. Gruner. 1985. Lyotropic effects of alkanes and headgroup composition on the L_α–H_{II} lipid liquid crystal phase transition: hydrocarbon packing versus intrinsic curvature. *J. Physique.* 46:761–769.
12. Seddon, J. M., G. Cevc, and D. Marsh. 1983. Calorimetric studies of the gel-fluid (L_β–L_α) and lamellar-inverted hexagonal (L_α–H_{II}) phase transitions in dialkyl and diacylphosphatidylethanolamines. *Biochemistry.* 22:1280–1289.
13. Evans, D. F., E. W. Kaler, and W. J. Benton. 1983. Liquid crystals in a fused salt: β, γ-distearoylphosphatidylcholine in N-ethylammonium nitrate. *J. Phys. Chem.* 87:533–535.
14. Nave, C., J. R. Helliwell, P. R. Moore, A. W. Thompson, J. S. Morgan, R. J. Greenall, A. Miller, S. K. Burley, J. Bradshaw, W. J. Pigram, W. Fuller, D. P. Siddous, M. Deutsch, and R. T. Tregear. 1985. Facilities for solution scattering and fibre diffraction at the Daresbury SRS. *J. Applied Crystallography.* 18:396–403.
15. Helliwell, J. R., T. J. Greenough, P. D. Carr, S. A. Rule, P. R. Moore, A. W. Thompson, and J. S. Morgan. 1982. Central data collection facility for protein crystallography, small angle diffraction and scattering at the Daresbury Laboratory Synchrotron Radiation Source (SRS), England. *J. Physics.* E15:1363–1372.
16. Bunn, C. W., and E. R. Howells. 1954. Structure of molecules and crystals of fluorocarbons. *Nature (Lond.).* 174:549–551.
17. Levine, Y. K. 1973. X-ray diffraction studies of membranes. *Prog. Surf. Sci.* 3:279–351.
18. Harlos, K. 1978. Pretransition in the hydrocarbon chains of phosphatidylethanolamines: a wide angle x-ray diffraction study. *Biochim. Biophys. Acta.* 511:348–355.
19. Tenchov, B. G., A. I. Boyanov, and R. D. Koynova. 1984. Lyotropic polymorphism of racemic phosphatidylethanolamine. A differential scanning calorimetry study. *Biochemistry.* 23:3553–3558.
20. McIntosh, T. J. 1980. Differences in hydrocarbon tilt between hydrated phosphatidylethanolamine and phosphatidylcholine bilayers: a molecular packing model. *Biophys. J.* 29:237–245.
21. Hentscherl, M. P., S. Braun, R. Dietrich, and L. Trahms. 1985. NMR and x-ray investigation of the phase behavior of phosphatidylethanolamines. *Mol. Cryst. Liq. Cryst.* 124:205–217.
22. Wilkinson, D. A., and J. F. Nagle. 1981. Dilatometry and calorimetry of saturated phosphatidylethanolamine dispersions. *Biochemistry.* 20:187–192.
23. Wittebort, R. J., A. Blume, T.-H. Huang, S. K. Das Gupta, and R. G. Griffin. 1982. Carbon-13 nuclear magnetic resonance investigations of phase transitions and phase equilibria in pure and mixed phospholipid bilayers. *Biochemistry.* 21:3487–3502.
24. O'Leary, T. J. and I. W. Levin. 1984. Effects of solvent on biomembrane structure: raman spectroscopic investigation of dipalmitoylphosphatidylcholine dispersed in N-ethylammonium nitrate. *J. Phys. Chem.* 88:4074–4078.